RESEARCH PAPER

PCCP

www.rsc.org/pccp

Structure determination of thiacyanine dye J-aggregates in thin films: Comparison between spectroscopy and wide angle X-ray scattering

G. Busse, B. Frederichs, N. Kh. Petrov and S. Techert*

Max-Planck-Institute for Biophysical Chemistry, Dept. of Spectroscopy and Photochemical Kinetics, 37070, Göttingen, Germany. E-mail: stecher@gwdg.de

Received 9th January 2004, Accepted 10th March 2004
First published as an Advance Article on the web 27th April 2004

The structural properties of J-aggregates in thin films were studied by wide-angle synchrotron X-ray scattering, UV/VIS absorption and fluorescence spectroscopy and time-correlated single photon counting. The system of investigation was the cyanine dye $(C_{33}H_{32}N_2O_6S_4^-{\cdot}HN(CH_2CH_3)_3^+$; 2-{3-[1-(3-sulfopropyl)-naphtho-[1,2-d]thiazol-2(1H)-yliden]-2-ethyl-1-propen-1-yl}-1-(3-sulfo-propyl)-naphtho-[1,2-d] thiazolium-betain·triethylammonium salt) incorporated into a Na-polystyrene-sulfonate (PSSNa) matrix. It could be shown that, depending on the preparation conditions, it is possible to create either a monomer phase or a J-aggregate phase in PSSNa films. Both could optically be distinguished through their typical bathochromic shift of the J-aggregate band in the UV/VIS spectra. Wide angle X-ray scattering experiments confirm intermolecular distances of 7 Å in the J-aggregate and an angle of inclination of 20°. Out of optical studies, the angle of inclination was determined to be around 30°. A more detailed interpretation of the wide angle X-ray scattering signals suggests that 80% of the formed J-aggregate consists of dimers and 20% of a helical arrangement with a diameter of *ca.* 16 Å. The used stacking model was built out of mono-*cis* conformer units which were confirmed to be the most stable conformation by DFT calculations (6-31G* basis set, BeckeLyp functional).

Introduction

The last decades have seen a growing interest in the study of the extraordinary spectral properties of cyanine dyes that are able to undergo photo-isomerisation and produce molecular aggregates.[1–5] Cyanine dyes are widely applied to photographic processes as spectral sensitizers making use of the sharp exciton absorption of J-aggregates in the red wavelength range. Their ability of undergoing coherent excitations made them a possible candidate for organic nonlinear materials.[4]

Though many methods concern detailed spectroscopic investigations of dye aggregates,[1–11] only a few X-ray scattering and scattering experiments were undertaken in order to determine the structure of these aggregates in aqueous solution[12] and to determine the monomer structure in crystals.[13] The purpose of this work is to study the structural properties of dye aggregates in thin films as derived by X-ray scattering methods, *i.e.* wide-angle X-ray scattering, and compare them with optical spectroscopic results, *i.e.* absorption and emission spectra and fluorescence lifetimes. For thus investigations, we have chosen a typical cyanine dye, $C_{33}H_{32}N_2O_6S_4^-{\cdot}HN(CH_2CH_3)_3^+$; 2-{3-[1-(3-sulfopropyl)-naphtho-[1,2-d]thiazol-2(1H)-yliden]-2-ethyl-1-propen-1-yl}-1-(3-sulfo-propyl)-naphtho-[1,2-d] thiazoliumbetain·triethylammonium salt (**CD1**), incorporated into a Na-polystyrene-sulfonate matrix (structure of **CD1**$^-$, see Fig. 1). Na-polystyrene-sulfonate (PSSNa) was reported as film material, which does not support the formation of J-aggregates.[14] However, in this work we could show that this assumption is not valid in general, and that it is possible to form **CD1** J-aggregates in PSSNa, strongly depending on the preparation conditions.

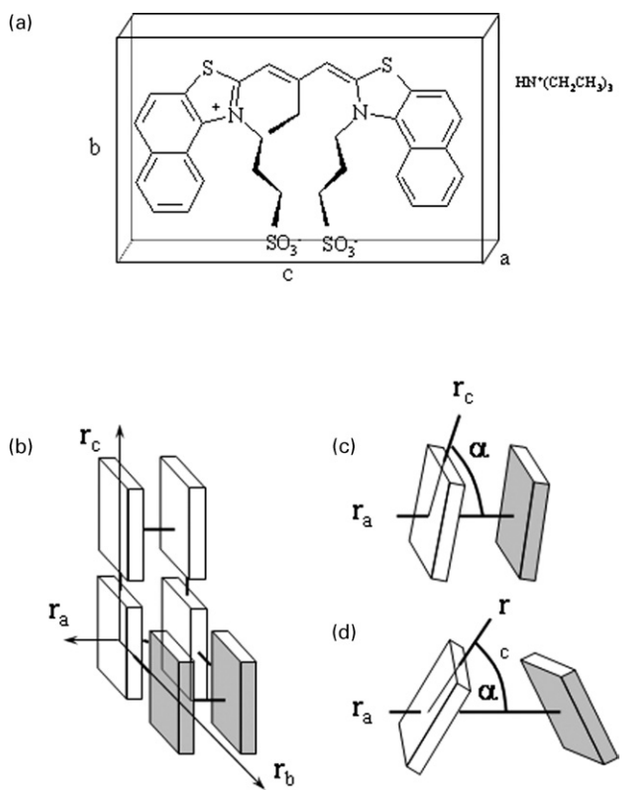

Fig. 1 (a) Structure and geometrical definition of the dye anion **CD1**$^-$ ($C_{33}H_{32}N_2O_6S_4^-$;2-{3-[1-(3-sulfopropyl)-naphtho-[1,2-d]thiazol-2(1H)-yliden]-2-ethyl-1-propen-1-yl}-1-(3-sulfopropyl)-naphtho-[1,2-d]thiazoliumbetain). (b) Definition of the stacking axis and intermolecular distances. (c) and (d) Summarise possible stacking for J and H-aggregates: (c) in-plane inclined configuration and (d) oblique configuration.

Experimental section

Sample preparation

The structure of the investigated dye anion **CD1**$^-$ is shown in Fig. 1a) with $HN(CH_2CH_3)_3^+$ as the counter cation. The dye

DOI: 10.1039/b400212a

(Sigma Aldrich) was re-crystallised and checked by UV absorption and emission spectroscopy. For optical measurements, the poly-Na-4-styrenesulfonate film (MW *ca.* 70 000, Sigma Aldrich) with dye concentration of 10^{-1} M were prepared by spin-coating techniques (500–900 rpm) on 1 mm thick quartz plates (Heraeus) or on microscope objective glass (Marienfeld). A mixture of methanol (Uvasol, Merck) and bidestilled water was used as a solvent. The plates were dried at 50° C for 30 s.

By applying the spin coating technique, phase aggregation of the film/dye mixture in two different phases has been observed: during the rotation of the objective glass, the sulfonate film spreads over the plate forming a blue film (as inner circle) surrounded by a pink film outer circle. As will be discussed in the following paragraph, the inner blue film part was assigned to the monomer phase of **CD1**$^-$ and the outer film circle to a J-aggregate phase. The film thickness was measured using a Dektak IIA (Sloan) profilemeter. For this work, films with thicknesses of 0.3 ± 0.02 μm for the monomer phase and 0.5 μm $\pm$ 0.09 μm for the J-aggregate phase were used.

For the X-ray scattering experiments the saturated dye-film solutions were spin-coated on glass plates, dried, each of the phases was scraped off the glass, grained and filled in a capillary.

Stationary and time-resolved optical spectroscopy

The stationary absorption spectra have been measured by a Cary-5E spectrometer. A Jobin-Yvon SPEX Fluorolog 3 fluorescence spectrometer was used to record the stationary quantum-corrected fluorescence spectra. In order to exclude re-absorption artefacts, the fluorescence spectra were measured in front-face geometry. In the wavelength range 250–800 nm the band-passes of the UV absorption and emission spectrometer were 0.5 nm, resulting in a resolution of 55 cm^{-1} at 350 nm.[15]

The fluorescence quantum yield of **CD1**$^-$ was determined for the films as well as for aqueous solution. As reference 10^{-5} M solution of oxazin 1 (Lambda Physics) in etOH (Merck, spectroscopic grade) was used.[16,17] The quantum yield was calculated according to the standard procedure taking into consideration the various optical densities and the changes in the refractive index of the different solvents.[18]

Fluorescence decay curves were recorded by a time-correlated single photon counting apparatus (TSCPC, Edinburgh Instruments) with a microchip Nd : YAG laser (Uniphase, 355 nm excitation wavelength, 80 ps time resolution) as excitation source. The data were analyzed by a deconvolution technique and fitted with a non-linear least-squares method based on the Levenburg–Marquard algorithm to mono- and multi-exponential decays, *i.e.* $\sum_i A_i \exp(-t/\tau_i)$. All TSCPC measurements were carried out at room temperature. The monomer decay curves were measured with a 550 nm interference filter (Melles Griot) and the J-aggregate decay curves were collected with a 650 nm cutoff filter (Schott).

Wide-angle X-ray scattering (WAXS)

Wide angle X-ray data were collected at the ID09B beamline of the European synchrotron radiation facility (ESRF). The polychromatic beam was produced by a 162 pole undulator in a 20 mm magnetic period ($K = 0.273$). The wavelength of the U20 undulator beam was selected to $\lambda_{X\text{-ray}} = 0.753$ Å ($E_{X\text{-ray}} \approx 16.5$ keV) by a Si_{111} monochromator (focus at the sample = 200×200 μm^2).[19] Scattering data were collected with a MAR133 CCD camera (diameter = 133 mm, pxl-size = 64.7×64.7 μm^2). Differently resolved wide-angle X-ray scattering measurements were reached by varying the sample-to-detector distance from 80 to 260 mm in 20 mm steps. Film samples were sealed in a glass capillary of 300 μm diameter and measured in transmission geometry. The WAXS experiments were carried out at room temperature. One-dimensional scattering patterns were obtained by integrating the two-dimensional images with Fit2d.[20] After integration and sufficient normalisation against the background signal and high q values, the 2-dimensional scattering pattern of the dye in the film material was subtracted from the scattering pattern of the pure film. Further data treatment was undertaken using home-written software.

Results and discussion

Characterisation of the different photoactive species *via* optical spectroscopy

Fig. 2 shows the absorption and emission spectra of the two phases of **CD1** incorporated in a PSSNa film. In the top part of Fig. 2, the absorption and emission spectra of the monomer phase are plotted. In the bottom part of Fig. 2, the corresponding spectra of the J-aggregate phase are shown. The monomer absorption spectrum (solid line) at the left hand side of Fig. 2, top, has an overall absorption maximum at $\lambda_{max}(\text{mono}) = 575$ nm. The absorption band can well be fitted through two Voigt profiles m1 and m2 (dotted lines) with two maxima at $\lambda_{max}(\text{m1}) = 554$ nm and at $\lambda_{max}(\text{m2}) = 613$ nm indicating that the $S_1 \leftarrow S_0$ transition (band m1) is at 554 nm

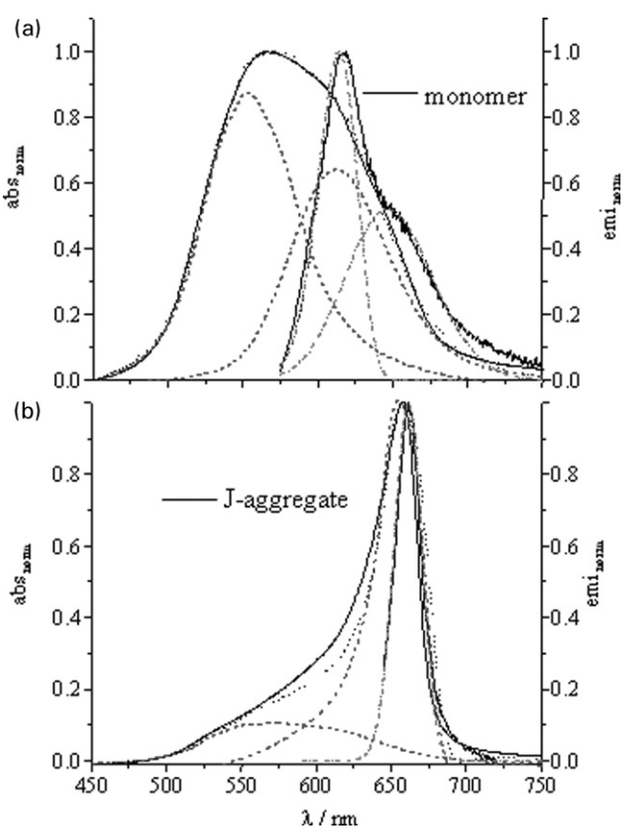

Fig. 2 Absorption spectra of the monomer and the J-aggregate spectrum of the thiacyanine dye **CD1**$^-$ in PSSNa films (c(dye) = 10^{-1} M). Top: absorption (left hand side) and emission spectrum (right hand side) of the monomer phase. The absorption band of the monomer can be fitted as a convolution of two absorption bands. The emission band of the monomer can only be refined with two log normal functions with essentially no asymmetry (small asymmetry factor). Bottom: absorption (left hand side) and emission spectrum (right hand side) of the J-aggregate phase. The absorption spectrum of the J-aggregate consists of the J-aggregate and small amounts of monomer (<10%). With an excitation beyond 625 nm, only the emission band of the J-aggregate has been found.

Table 1 The properties of the absorption band of the monomer (m) and the J-aggregate (J-agg). The absorption band of the monomer can be fitted as a convolution of two absorption bands, called m1 and m2 in Fig. 2, top. The absorption spectrum of the J-aggregate consists of the J-aggregate and small amounts of monomer (<10%)

	ν^{abs}_{max}/cm^{-1}	$\Delta\nu^{abs}_{fwhm}/cm^{-1}$	$\varepsilon_{max}/l\ mol^{-1}\ cm^{-1}$	f_{osc}	$\lvert R_{mn}\rvert^2/D^2$	τ_{calc}/ns	$\tau_{calc}*\Phi_{fl}/ns$
m1	18 063	2391	94 720	1.310	147.8	3.22	0.322
m2	16 324	2034.5	94 720	0.216	26.8		
J	15 315	833	140 500	0.446	61.5	15.1	1.41

or even at lower energies. The bandwidth of the monomer absorption band is found to be $\Delta\nu_{fwhm}(m1) = 2035\ cm^{-1}$ and $\Delta\nu_{fwhm}(m2) = 2391\ cm^{-1}$. The molar extinction coefficients for the monomer spectrum was determined to be $\varepsilon_{575\ nm}(mono) = 94\,720\ l\ mol^{-1}\ cm^{-1}$. The measured emission spectrum of the monomer phase (right hand side, solid line) has an emission maximum at $\lambda_{max}(mono) = 618$ nm. It can only be fitted through two log-normal functions (m1′ and m2′) with two band maxima at $\lambda_{max}(m1') = 648$ nm and at $\lambda_{max}(m2') = 614$ nm and $\Delta\nu_{fwhm}(m1') = 1632\ cm^{-1}$ and $\Delta\nu_{fwhm}(m2') = 770\ cm^{-1}$ bandwidth, respectively. The asymmetry factor is close to 0.5 (essentially no asymmetry of the two fitted bands). The fluorescence quantum yield of the monomer was determined to be $\Phi_f(mono) = 0.1$. The characteristic properties of the absorption and emission bands are summarized in Table 1.

Fig. 2, bottom, shows the absorption and emission spectra of the J-aggregate phase obtained in the same sample at another spatial location of the film (outer circle). According to the technique described in the experimental section, on the same sheet of sample with the same dye concentration two different phases of **CD1**$^-$ are created, which are spatially well separated. The found absorption band (left hand side) has a band maximum at $\lambda_{max} = 656$ nm. Since the found narrowband species has a similar absorption spectrum to that of **CD1**$^-$ in water, it has been assigned to a J-aggregate—in consistence with ref. 21. The bandwidth of the J-aggregate is $\Delta\nu_{fwhm}(J-agg) = 833\ cm^{-1}$ (see also Table 1). The extinction coefficient was found to be at $\varepsilon_{656\ nm}(J-agg) = 140\,500\ l\ mol^{-1}\ cm^{-1}$. On the right hand side of Fig. 2, bottom, the emission spectrum of the J-aggregate of **CD1**$^-$ in PSSNa is shown. With an excitation beyond 625 nm, only the emission band of the J-aggregate has been found with a peak maximum at $\lambda_{max}(J-agg) = 663$ nm and with a FWHM of $\Delta\nu_{fwhm}(J-agg) = 501\ cm^{-1}$. The fluorescence quantum yield of the J-aggregate was determined to be $\Phi_f(J-agg) = 0.12$ (Table 2).

It should be pointed out that both phases are created within the same sample at the same dye concentration but at different well-separated spatial positions on the film by applying the spin-coating technique at optimized rotation speed, as described in the previous paragraph. However, as indicated by the spectra, the separation into the monomer phase and the J-aggregate phase is not fully possible. In the monomer phase the ratio of $n(mono):n(J-agg)$ was found to be 9.5 : 0.5 and 1 : 9 for the J-aggregate phase.

Table 2 The emission band of the monomer can only be refined with two log normal functions (m1′ and m2′) with essentially no asymmetry (small asymmetry factor). Since both emission bands have different full width at half maximum values they probably belong to two different fluorescent states (or species). M2′ is probably the monomer emission and m1′ is the emission occurring from an aggregate. With an excitation beyond 625 nm, only the emission band of the J-aggregate has been found

	ν^{fl}_{max}/cm^{-1}	$\Delta\nu^{fl}_{fwhm}/cm^{-1}$	Φ_f	τ_f/ns
Monomer				
m1′	15 434	1632	0.10	0.400
m2′	16 274	770		
J-aggregate				
J	15 092	501	0.12	0.520

In addition to these stationary experimental results, the fluorescence lifetimes of the monomer phase and the J-aggregate phase were separately measured by TCSPC (see Table 2). All fluorescence decay curves could mono-exponentially be fitted. The fluorescence lifetimes were determined to $\tau_f(mono) = 400$ ps and $\tau_f(J-agg) = 520$ ps (Table 2).

In the literature a lot of work has been undertaken in order to understand how J-aggregates influence their characteristic spectroscopic features. Theoretical considerations as well as detailed spectroscopic studies suggest a strong relationship between structure—namely the stacking geometry of the molecules—and the spectroscopic properties. For example, the absorption spectrum of the chromophores can be used in order to elucidate the unperturbed, natural fluorescence lifetimes of the chromophores. The method has been developed by Strickler and Berg[22] and is applicable if, within the limits of the Franck–Condon principle, the absorption and emission spectra are mirror images of each other (microscopic reversibility). Following a procedure suggested in ref. 16, the natural fluorescence lifetimes of $\tau_{calc}(J-agg) = 15.1$ ns and $\tau_{calc}(m1) = 3.2$ ns, respectively, are estimated (Table 1). These values reflect the inverse proportionality of the oscillator strength f_{osc} to the natural fluorescence lifetime τ_{calc}. For the J-aggregate, the oscillator strength is dominated by the small bandwidth of the absorption band compared to the monomer band explaining why τ_{calc} for the monomer is so much smaller in comparison to the J-aggregate ones. Experimentally, also the J-aggregate fluorescence shows a higher value than the ones for the monomer. However, a comparison between the calculated, natural fluorescence lifetimes τ_{calc} and the true measured ones τ_f has a qualitative rather than quantitative character: in the case of the monomer, τ_{calc} and τ_f are comparable though they differ by a factor of 2 for the J-aggregate. This suggests that the process of J-aggregation, in particular, is a more complex process than the one described in a simple two state model for the J-aggregate phase. Nonetheless, it should be mentioned that in the case of rhodamine dyes[23] the experimental fluorescence lifetime increases with increasing J-aggregation. It was explained by the rise of fluorescing J-aggregate concentration and a decrease of fluorescence-quenching H-aggregates.

From the bandwidth of the absorption spectra it is possible to determine the coherent size N_{J-agg} of the Frenkel excitons in a J-aggregate[4–8] according to

$$\Delta\nu_{fwhm}(mono)/\Delta\nu_{fwhm}(J-agg) = \sqrt{N_{J-agg}} \qquad (1)$$

Knowing the fluorescence quantum yield Φ_f (Table 2), it is alternatively possible to obtain the coherence length by knowing the kinetic constants of the fluorescence[6,11]

$$k_f(mono) = N_{J-agg}k_f(J-agg) \qquad (2)$$

with $k_f = \Phi_f/\tau_{calc}$. With eqn. (1) it is found that $N_{J-agg} = 3$ and with eqn. (2) $N_{J-agg} = 4$, respectively. Note that for the

calculation the natural fluorescence lifetime was used, which presents the non-perturbed case.

In order to elucidate structural features of the aggregate out of the spectroscopic data, the stacking geometry of the chromophors or, in other words, the relative orientation of the transient dipole moment of each molecule to each other in the aggregate has to be studied. In order to simulate the arrangements of the dye aggregates we used a simple geometrical model, as shown in Fig. 1. It is assumed that one **CD1**$^-$ anion unit can be considered as some kind of rectangular solid with the edge lengths a, b, and c (Fig. 1a). The monomers assembly as aggregates in different stacks (Fig. 1b), where the intermolecular distances between the anions are defined as r_a, r_b and r_c. Since the anions can be tilted and rotated against each other, the geometry of one dye dimer (Figs. 1c and 1d) is further defined by two angles, the angle of inclination α and the angle of rotation γ. α spans the angle between one molecular axis (*i.e.* the monomer transition-dipole moment) and one stacking axis of the aggregate. As is commonly accepted,[1–6] J-dimers are defined with stacking angles $\alpha < 54.7°$ and H-dimers with those angle values of $\alpha > 54.7°$. γ is related to α by $\alpha + 2\gamma = 180°$. In the absorption spectra, H-aggregates occur blue shifted with respect to the monomer spectrum and J-aggregates red-shifted.

Since the transition dipole moment is directly proportional to the transition probability $|R_{mn}|^2$, it is possible to estimate

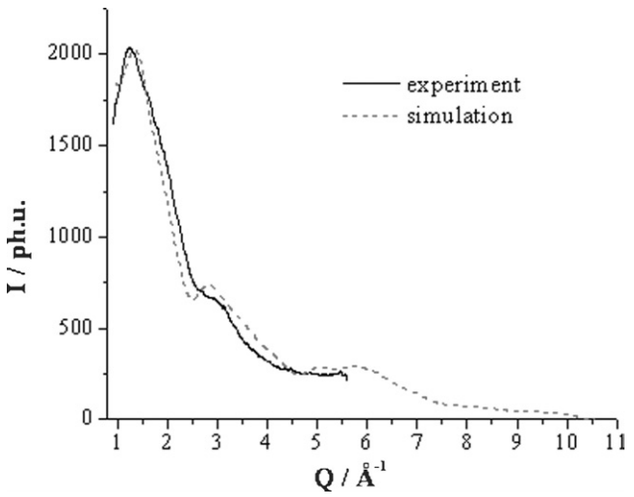

Fig. 3 Amorphous wide-angle X-ray scattering of the J-aggregate phase of the **CD1** dye in PSSNa film (after subtraction of the pure PSSNa film signal) with c (dye) $> 10^{-1}$ M. $Q = 2\pi\sin\Theta/\lambda$ with $\lambda(U20) = 0.753$ Å. A characteristic maximum of the scattered X-ray intensity at low Q values is found as a consequence of the aggregation (and clusterisation). The simulated X-ray signal based on the models following is shown as a dashed line.

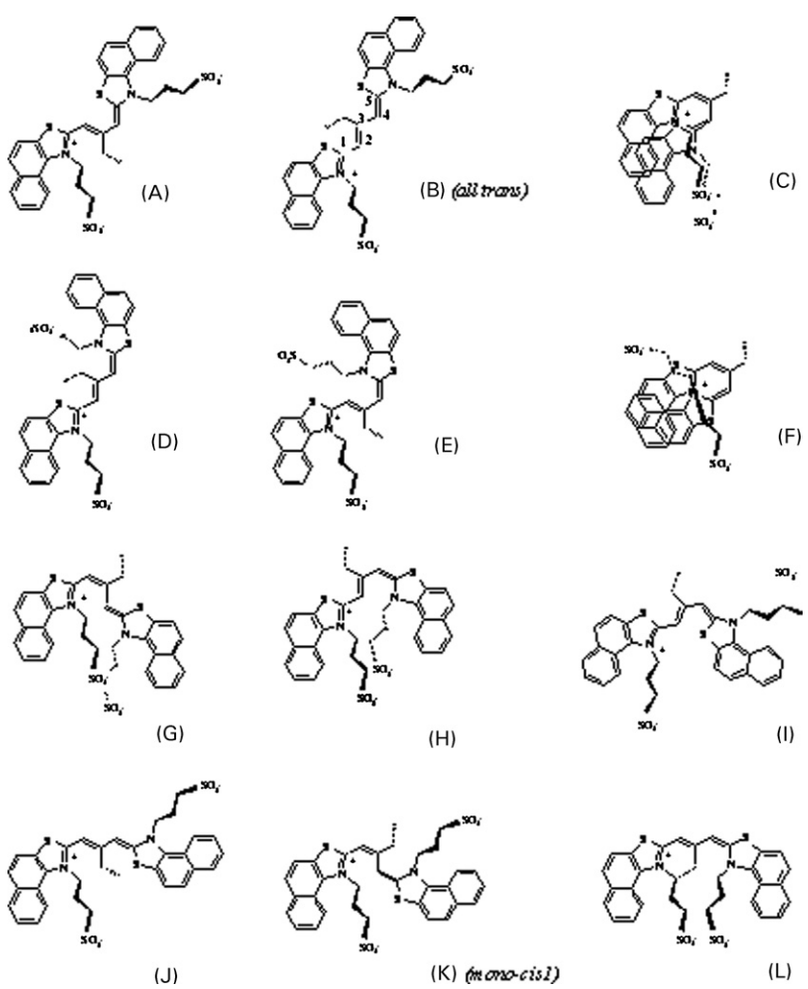

Fig. 4 The possible 12 configurations of **CD1**$^-$. The configurations can be distinguished according to syn/anti ordering of the N/S aromatic moieties and/or according to the *cis*/*trans* configurations around the three mesomeric double bonds (1–5 in configuration **B**). Note, that the configurations **A** ↔ **B**, **D** ↔ **E**, **G** ↔ **H** and **J** ↔ **K** can be interconverted by a hula-twist mechanism. According to DFT calculations (RLYP3B, 6-31G* basis set) the most stable configuration is the *mono-cis1* configuration **K** followed by the *all-trans* configuration **B**. **C** and **F** are the most unfavourable and less stable configurations.

the angle of inclination α from the spectroscopic properties of the absorption and emission spectrum, namely the coherence length which has been derived according to eqns. (1) and (2)[11]

$$1/\sqrt{N_{\mathrm{J-agg}}} = \cos^2(\alpha) \qquad (3)$$

Taking the found values, the angle of inclination of the J-aggregate, α, was found to be between 30 and 35°. The angle of rotation $\gamma = (180° - \alpha)/2$ ranges consequently from 60 to 65°.

Wide angle X-ray scattering (WAXS) studies of the J-ggregate phase

By means of optical steady-state and time-resolved spectroscopy, it is possible to determine approximately the principle stacking geometry of the dye aggregate as well as the angle of inclination. However, for additional detailed information about the size and shape of an aggregation unit, other independent methods are required. Therefore we applied an X-ray base method, wide angle X-ray scattering (WAXS). WAXS provides information about the pair distance distribution function and the electron density distribution function of amorphous bodies, which can be correlated with the intermolecular distances to the nearest neighbors,[24,25] an important parameter for the structure of **CD1**$^-$ J-aggregates.

Fig. 3 shows the measured WAXS signal of the J-aggregate phase (solid line) after subtraction from the pure PSSNa film signal. The scattered intensity is plotted as a function of $Q = 4\pi\sin\theta/\lambda$ in Å^{-1}. Two distinguished signal maxima are found which correspond to two maxima in the pair distance distribution function of $r = 2$–3 Å and $r = 6$–7 Å.

In order to simulate the X-ray signal for different J-aggregate compositions, one has to first define the geometry of one monomer unit. For **CD1**$^-$, the structural parameters of a monomer are not experimentally known. Therefore the structure of one **CD1**$^-$ monomer unit was simulated by DFT (RLYP3B) calculation using the 6-31G* basis set (Gaussian package[26–29]). Indeed, the structure of **CD1**$^-$ is of more complexity, since one can distinguish 12 conformers, as they are shown in Fig. 4. The configurations can be distinguished according to syn/anti ordering of the N/S aromatic moieties

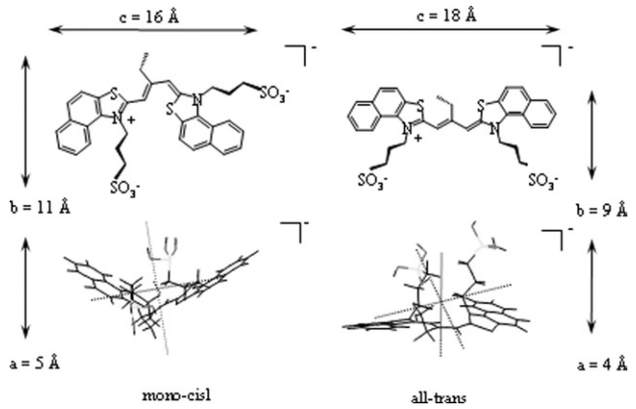

Fig. 5 Geometrical parameters of the *mono-cis1* (**K**) and the *all-trans* (**B**) configuration of **CD1**$^-$. The structural differences of both configurations are too small to be resolved in the present WAXS study on J-aggregate films.

and/or according to the *cis*/*trans* configurations around the three mesomeric double bonds (1–5 in configuration **B**). Note, that the configurations **A** ↔ **B**, **D** ↔ **E**, **G** ↔ **H** and **J** ↔ **K** can be converted by a hula-twist mechanism. According to the DFT calculations, the most stable configuration is the *mono-cis1* configuration **K** followed by the *all-trans* configuration **B**. **C** and **F** are the most unfavourable and less stable configurations. Though the DFT calculation were done on a single molecule assuming no external forces (gas phase conditions), the most stable structure coincides with the crystal structure of a similar compound,[13] where the *mono-cis1* configuration was also the one determined to form the crystal lattice (and therefore obviously the most stable one).

Indeed, as shown in Fig. 5, the structural differences of the two most stable configurations of **CD1**$^-$ *mono-cis1* (K) and the *all-trans* (B), are too small to be resolved in the present WAXS study on J-aggregate films. However, as can be seen by the side view of the chromophors (Fig. 5, bottom), the *mono-cis1* configuration is not as planar as the *all-trans* configuration influencing the aggregation stacking geometry. The stacking model of the J-aggregate is based on the *mono-cis1* configuration of CD1$^-$ with varying angle of inclination and

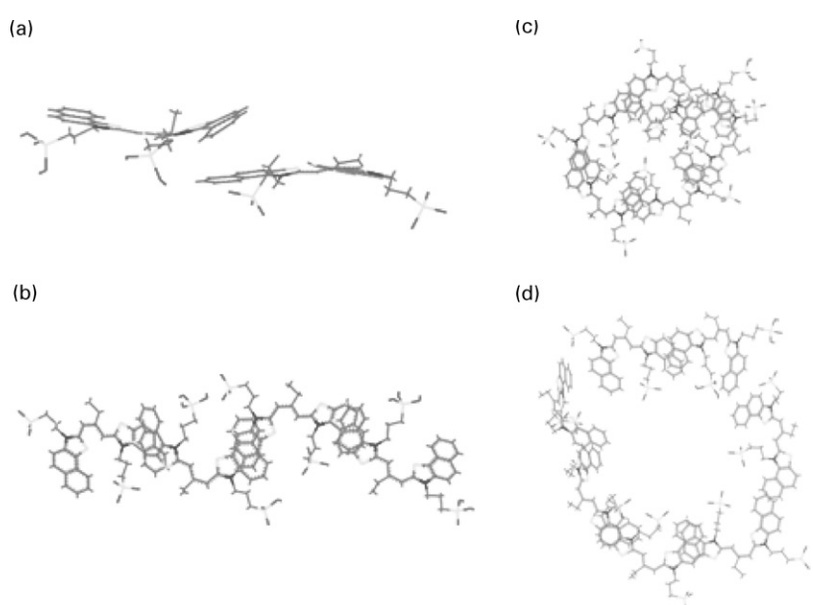

Fig. 6 Different stacking models for the J-aggregate. The used monomer unit is the *mono-cis1* configuration of **CD1**$^-$. Fig. 6a shows a dimer unit from which the aggregates were built. Fig. 6b presents the used chain model with alternating head–tail configurations. In Fig. 6c and 6d two helical arrangements with different helical diameter extremes are shown for $d = 12$ Å (minimum, Fig. 6c) and $d = 20$ Å (maximum, Fig. 6d). The **CD1**$^-$ units stack in such a way that one aromatic residue of the **CD1**$^-$ moiety aggregates with another aromatic moiety of another **CD1**$^-$ moiety.

varying stacking geometry. Fig. 6a shows a dimer unit from which the aggregates were built.

As aggregate model three basic configurations were used: first, the chain model (Fig. 6b) with alternating head–tail configurations of **CD1**$^-$ and, secondly, two helical arrangements with different helical diameter. As two extremes of such configurations in Fig. 6 the helical arrangement for $d = 12$ Å (minimum, Fig. 6c) and $d = 20$ Å (maximum, Fig 6d)) are shown. The refined helical rearrangement started at the minimum diameter and was increased to the maximum diameter in steps of one **CD1**$^-$ unit resulting in a diameter increase of *ca*. 3 Å. Here, the **CD1**$^-$ stacks in such a way that one aromatic residue of the **CD1**$^-$ moiety aggregates with another aromatic moiety of another **CD1**$^-$ moiety. The best coincidence between model experimental WAXS data was found for 80% of dimer contribution and 20% of aggregate contribution with a helical arrangement and a diameter of $d = 16$ Å. The best fitted angle of inclination was found to be $\alpha = 18°$ which is slightly smaller than the angle of inclination determined by spectroscopy (30°).

Conclusion

It was found that, contrary to claims in literature, J-aggregation can be found in PSSNa films. In order to determine precisely the nature of the J-aggregation, steady-state and time-resolved optical studies, as well as wide angle X-ray scattering studies, have been performed. Their results lead to complementary information about the structure of the J-aggregates of **CD1**$^-$ thiacyanine dyes in poly-Na-4-styrene-sulfonate thin film material. The former are sensitive against the intermolecular tilt angles—the angle of inclination α and the angle of rotation γ—and the latter determine intermolecular distances and stacking geometries. Applying both fields of techniques can result in a complete picture about the features of J-aggregation of **CD1**$^-$. It was found that the angle of inclination for J-aggregates of **CD1**$^-$ embedded in charged films ranges between 20° (WAXS studies) and 30° (optical results). The molecular distances to the nearest neighbors show two dominant distribution function maxima at 3 and 7 Å, respectively. Based on the model developed out of DFT calculations (on the monomer units), the experimental WAXS signal on the J-aggregate could best be fitted by 80% of dimer contribution and 20% of helical arrangement with a diameter of $d = 16$ Å. DFT simulations support that the *mono-cis* configuration is the most stable configuration of cyanine dyes, substituted at the 3-*meso* position.

Acknowledgements

The authors wish to thank J. Bienert (MPI) and A. Plech (ESRF) for their technical support. Prof. M. Wulff and Prof. J. Troe are thanked for their permanent support and interest in this work. The authors are grateful to DFG for the research grant TE 347/1-2 and the Aventis Foundation. N. Kh. P. thanks the Max Planck Society and the DFG (436 RUS 113/755/1-1) for support.

References

1 G. Scheibe, *Angew. Chem.*, 1936, **50**, 51.
2 E. E. Jelley, *Nature (London)*, 1936, **138**, 1009.
3 K. H. Drexhage, M. M. Zwick and H. Kuhn, *Ber. Bunsen-Ges. Phys. Chem.*, 1963, **67**, 62.
4 H. Kuhn and D. Möbius, *Angew. Chem., Int. Ed. Engl.*, 1971, **10**, 620.
5 D. Möbius, *Adv. Mater.*, 1995, **5**, 437.
6 (*a*) E. G. McRae and M. Kasha, *J. Chem. Phys.*, 1958, **28**, 721; (*b*) M. Kasha, M. A. El-Bayoumi and H. R. Rawls, *Pure Appl. Chem.*, 1965, **11**, 371.
7 P. Weidner and A. Penzkofer, *Chem. Phys.*, 1995, **191**, 303.
8 E. W. Knapp, *Chem. Phys.*, 1984, **85**, 73.
9 M. R. V. Sahyun and N. Serpone, *J. Phys. Chem.*, 1997, **101**, 9877.
10 N. Kometani, H. Nakajima, K. Asami, Y. Yonezawa and O. Kajimoto, *J. Phys. Chem.*, 2000, **104**, 9630.
11 K. Kemnitz, N. Tamai, I. Yamazaki, N. Nakashima and K. Yoshihara, *J. Phys. Chem.*, 1986, **90**, 5094.
12 W. J. Harrison, D. L. Mateer and G. J. T. Tiddy, *J. Phys. Chem.*, 1996, **100**, 2310.
13 H. Stoeckli-Evans, *Helv. Chim. Acta*, 1974, **57**, 1.
14 A. H. Herz, R. P. Dauner and G. A. Janusonis, *Advances in Chemistry*, ACS, Washington, DC, 1968, 79, p. 173.
15 (*a*) S. Techert, S. Schmatz, A. Wiessner and H. Staerk, *J. Phys. Chem. A*, 2000, **104**, 5700; (*b*) S. Techert, A. Wiessner, S. Schmatz and H. Staerk, *J. Phys. Chem. B*, 2001, **105**, 7579.
16 L. F. Vieira Ferreira and S. M. B. Costa, *J. Lumin.*, 1991, **48/49**, 395.
17 K. H. Drexhage, *Structure and Properties of Laser Dyes*, *Topics in Applied Physics*, ed. F. P. Schäfer, Springer Series, Berlin, 1979, vol. 1, 147–152, 171–172.
18 W. H. Melhuish, *Natl. Bur. Std.–Proc. Conf. NBS*, Washington, 1972, p. 378.
19 S. Techert, F. Schotte and M. Wulff, *Phys. Rev. Lett.*, 2001, **86(10)**, 2030.
20 (*a*) A. P. Hammersley, M. Svensson, M. Hanfland, A. N. Fitch and D. Haeussermann, *High Press. Res.*, 1996, **14**, 235; (*b*) A. P. Hammersley, S. O. Svensson and A. Thomson, *Nucl. Instrum. Methods Phys. Res., Sect. A*, 1994, **346**, 321.
21 L. Jeaunieau, V. Alin and J. B. Nagy, *Langmuir*, 2000, **16**, 597.
22 S. J. Strickler and A. Berg, *J. Chem. Phys.*, 1962, **37**, 814.
23 F. del Monte, M. L. Ferrer and D. Levy, *Langmuir*, 2001, **17**, 4812.
24 A. Guinier, *X-ray Scattering in Crystals and Amorphous Bodies*, Re-publication from 1963, Dover Publications, NY, 1994.
25 B. E. Waren, *X-ray Scattering*, Addison-Wesley, Reading, MA, 1969.
26 M. J. Frisch, G. W. Trucks, H. B. Schlegel, P. M. W. Gill, B. G. Johnson, M. A. Robb, J. R. Cheeseman, T. Keith, G. A. Petersson, J. A. Montgomery, K. Raghavachari, M. A. Al-Laham, V. G. Zakrzewski, J. V. Ortiz, J. B. Foresman, J. Cioslowski, B. B. Stefanov, A. Nanayakkara, M. Challacombe, C. Y. Peng, P. Y. Ayala, W. Chen, M. W. Wong, J. L. Andres, E. S. Replogle, R. Gomperts, R. L. Martin, D. J. Fox, J. S. Binkley, D. J. Defrees, J. Baker, J. P. Stewart, M. Head-Gordon, C. Gonzalez and J. A. Pople, *Gaussian 98 - Revision B.3*, Gaussian Inc., Pittsburgh, PA, 1998.
27 A. D. Becke, *J. Chem. Phys.*, 1993, **98**, 5648.
28 C. Lee, W. Yang and R. G. Parr, *Phys. Rev. B*, 1988, **37**, 785.
29 B. Miehlich, A. Savin, H. Stoll and H. Preuss, *Chem. Phys. Lett.*, 1989, **157**, 200.

